© 2020. Published by The Company of Biologists Ltd | Journal of Cell Science (2020) 133, jcs235838. doi:10.1242/jcs.235838

RESEARCH ARTICLE

Topical insulin application accelerates diabetic wound healing by promoting anti-inflammatory macrophage polarization

Peilang Yang[1,*], Xiqiao Wang[1,*], Di Wang[2,*], Yan Shi[1], Meng Zhang[1], Tianyi Yu[1], Dan Liu[1], Min Gao[1], Xiong Zhang[1,‡] and Yan Liu[1,‡]

ABSTRACT

Besides regulating glucose levels, insulin has been reported to participate actively in many other functions, including modulating inflammatory reactions. In this study we investigated how topical insulin application would affect the diabetic wound healing process. We found that the excessive expression of insulin-degrading enzyme led to insufficient insulin levels in diabetic skin during wound healing, which ultimately reduced the recovery rate of diabetic wounds. We confirmed that topical insulin application could reverse the impaired inflammation reaction in the diabetic wound environment and promote healing of diabetic wounds. Our study revealed that insulin promoted apoptosis of neutrophils and subsequently triggered polarization of macrophages. Both *in vivo* and *in vitro* studies verified that insulin re-established phagocytosis function and promoted the process of phagocytosis-induced apoptosis in neutrophils. Furthermore, we found that insulin treatment also promoted efferocytosis of the apoptosed neutrophils by macrophages, and thus induced macrophages to change their polarization state from M1 to M2. In conclusion, our studies proved that the exogenous application of insulin could improve diabetic wound healing via the restoration of the inflammatory response.

KEY WORDS: Diabetes, Wound healing, Insulin, Macrophages, Neutrophils

INTRODUCTION

Diabetes is a group of metabolic diseases characterized by polydipsia, polyphagia, polyuria, emaciation and weakness (American Diabetes, 2004), along with long-term complications such as diabetic nephropathy, diabetic retinopathy and lower extremity ulcers. Around 15–25% of diabetic patients experience diabetic foot ulcers during their lifetime (Leone et al., 2012).

Wound healing is a complex physiological event. The body's reaction to tissue injury involves various cells, cytokines and growth factors. Usually, this process is divided into hemostasis and inflammatory phases, a proliferative phase and a remodeling phase (Gurtner et al., 2008). Hemostasis and inflammation is the first chapter of wound healing, and neutrophils are the first nucleated cells that infiltrate into the wound after injury (Dovi et al., 2004). Once a wound is formed, the damaged tissue activates platelets, and numerous cytokines collectively recruit neutrophils to the wound site (Kolaczkowska and Kubes, 2013). The main functions of neutrophils are to maintain the aseptic environment by destroying invading microbes and to devitalize the tissue by secreting antimicrobial substances and proteases (Dovi et al., 2004; McCarty and Percival, 2013). A strong neutrophil response during the early stages after wounding benefits wound healing by controlling the infection and preparing wound beds. However, prolonged presence of neutrophils, combined with high amounts of proteases and reactive oxygen species (ROS) produced by neutrophils, which degrade growth factors and extracellular matrix, has harmful effects on healing (McCarty and Percival, 2013). As healing progresses, the pro-inflammation environment that induces infiltration of neutrophils needs to be depleted, and neutrophil infiltration needs be reduced progressively, such that inflammation resolution occurs gradually (Ortega-Gómez et al., 2013). Wound neutrophils proceed to apoptose, and subsequent macrophage polarization is the central step of inflammation resolution. The persistent presence of neutrophils or failure of resolution has been confirmed as the cause of chronic inflammation (Headland and Norling, 2015; Ortega-Gómez et al., 2013). Normally, circulating neutrophils experience constitutive apoptosis within 24 h and are engulfed in the liver, spleen and bone marrow (Li et al., 2011; Tofts et al., 2011; Pillay et al., 2010; McCracken and Allen, 2014). In inflammatory or injured sites, neutrophils may increase their lifespan, and eventually undergo apoptosis through the activation of phagocytosis-induced, TNF-α-induced or Fas-ligand-induced signaling pathways (Fox et al., 2010; McCarty and Percival, 2013). The apoptosed neutrophils release a number of substances that act as a 'find me signal' that attracts migrating macrophages and stimulates phagocytosis. Efferocytosis, the process of macrophage engulfment of apoptosed neutrophils, induces macrophage phenotype transformation from M1 to M2. The M2 macrophages secrete a number of cytokines and growth factors, such as IL-10, TGF-β, PDGF and VEGF, to promote the resolution of inflammation and induce the wound to transition to the proliferative stage of healing (Ortega-Gómez et al., 2013; Soehnlein and Lindbom, 2010; Ariel and Serhan, 2012).

Compared to neutrophils in the normal wound healing process, however, the functions of diabetic neutrophils, including adhesion to the endothelium, chemotaxis, phagocytosis and bactericidal activity, are all impaired (Alba-Loureiro et al., 2006). The dysfunction of inflammatory cells in the wound environment is the main pathological feature of diabetic wound healing. Impairment of macrophage polarization is the most significant and important such impairment, and is characterized by macrophages persisting in a pro-inflammatory phenotype (M1 phenotype). Macrophages are considered to be regulators of the wound healing process, because they manipulate wound healing through changing their polarization

[1]Department of Burns and Plastic Surgery, Shanghai Jiao Tong University, School of Medicine, Ruijin Hospital, Shanghai 200025, China. [2]Department of Anesthesiology, Shanghai No. 6 People's Hospital, Shanghai 200233, China.
*These authors contributed equally to this work

‡Authors for correspondence (rjliuyan@126.com; xiong@medmail.com.cn)

P.Y., 0000-0002-8648-782X; X.W., 0000-0002-2139-9853; D.W., 0000-0003-4414-8181; Y.S., 0000-0001-7517-8514; M.Z., 0000-0001-8647-1951; T.Y., 0000-0003-2286-8321; D.L., 0000-0001-8388-3512; M.G., 0000-0002-0001-5283; X.Z., 0000-0003-4828-2337; Y.L., 0000-0003-4242-228X

Handling Editor: Daniel Billadeau
Received 5 July 2019; Accepted 24 August 2020

Journal of Cell Science (2020) 133, jcs235838. doi:10.1242/jcs.235838

phenotype from M1 to the pro-healing M2 phenotype. This phenotype transformation occurs at the same time as the healing process switches from the inflammation phase to the proliferation phase. Many researchers intend to promote diabetic wound healing by targeting promotion of the impaired inflammatory phase.

Our previous work, and that of others, has proved that insulin not only acts as a glucose-regulating hormone but also as a growth-like factor and cytokine regulator that could accelerate wound healing in healthy non-diabetic rodents (Chen et al., 2012; Zhang et al., 2007). Many studies have revealed that insulin can regulate functions of neutrophils and macrophages that are impaired in the diabetic state. In recent years, others have reported that insulin application can also accelerate diabetic wound healing in type I diabetic rodent models (Lima et al., 2012). Type I diabetes is caused by the lack of insulin secretion, not by insulin resistance. It has been proven by researchers that supplementary insulin can enhance wound healing by reversing the effects of insufficient insulin. However, most diabetic non-healing wounds originate from type II diabetic wounds, which are characterized by insulin resistance and metabolic disturbances. Many of these patients are still in a state of high insulinemia. The effects of insulin application during the healing process of type II diabetic wounds are not well studied. Thus, in this article we thoroughly investigated the effects of a topical insulin treatment for type II diabetic wound healing and tried to understand the mechanisms behind these effects.

First, we established a diabetic rat model that has the major characteristics of type II diabetes, including insulin resistance and hyperinsulinemia (Yang et al., 2016). In order to compare how serum insulin and directly applied insulin affect the wound healing process, we further proved that the skin tissue of the type II diabetic rats were as sensitive as liver tissues to applied insulin stimulation (Yu et al., 2017). However, we further found a deficiency of insulin in both uninjured diabetic skin tissue and diabetic wounds, as compared to the non-diabetic wounds, where even the serum insulin level was relatively higher. In chronic wounds, elevated proteolytic enzyme activities, such as those of matrix metalloproteinases (MMPs) and serine proteases, have been detected (Muller et al., 2008; Loffler et al., 2013). The excessive wound proteases degrade the extracellular matrix, growth factors and/or their receptors; therefore leading to a deficient pool of growth factors in the wound area, which accordingly results in impaired healing (Wlaschek et al., 1997; McCarty and Percival, 2013). In recent years, some researchers have reported elevated insulin-degrading enzyme (IDE) activity in diabetic wounds (Tang, 2016). To reveal whether insulin deficiencies in the wound were caused by hyper IDE activity, we investigated IDE and insulin levels in the diabetic rat model. We found that the elevated activity of IDE could degrade insulin in local tissues and lead to an insulin-deficient state in tissues. This finding illustrates why the serum insulin level is still high, whereas the local wound area may be short of insulin stimulation, which manifests as diminished response of the local tissues to insulin stimulation. To solve the shortage of insulin stimulation in the local area of the wound, we studied the effects of topical insulin application on the healing of diabetic wounds and found that topical insulin application expedited the wound healing process by promoting macrophage polarization and transition to the M2 phenotype.

RESULTS

Insulin levels in diabetic skin and diabetic wounds are reduced due to overexpression of IDE in diabetic skin tissue

To investigate the expression of insulin in diabetic skin, we first compared the insulin level of uninjured skin tissue in normal and diabetic rats. A significantly lower insulin level (Fig. 1A,B) was detected in diabetic skin, despite the serum insulin level being higher in the diabetic rats, according to our previous studies (Yang et al., 2016). Further investigation of the insulin level during the wound healing process also confirmed the insufficiency of insulin in diabetic wounds (Fig. 1C,D). To reveal whether the insulin deficiency in the diabetic wounds was caused by elevated IDE activity, we further analyzed the IDE levels by ELISA, and assayed the distribution of IDE by immunohistochemistry (IHC). There were significantly higher IDE levels (Fig. 1E,G) and more extensive IDE distribution (Fig. 1F,H) found in diabetic skin and diabetic wounds compared to those in the normal skin and normal wounds. To further verify whether high IDE level could impact wound healing, we used the IDE inhibitor 6bK, which was applied to the diabetic wound topically combined with intraperitoneal injection. We found that diabetic wounds with IDE inhibitor application healed faster than the control diabetic group (Fig. 1I,J). The observations that high IDE level induced an insulin deficient state in diabetic skin and that IDE inhibitor could accelerate diabetic wound healing prompted us to test the effects of insulin supplement via topical application to the diabetic skin.

Topical insulin supplement promotes diabetic wound healing, macrophage infiltration and resolution

After confirming the insulin-deficient state of the diabetic skin and wound, we next investigated whether an extra insulin application could accelerate diabetic wound healing. We first examined insulin levels in both diabetic and insulin application groups. We found that insulin application significantly elevated wound insulin level in the insulin application group (Fig. 2A,B). We next set up our experiments, in which three groups were compared: the healthy normal rats as the standard group (Norm), the diabetic group without insulin treatment (DM) and the diabetic group with insulin treatment (DM+Ins). As one of the features to define the wound healing process, we recorded the healing time for the Norm, DM and DM+Ins groups. We found that insulin application efficiently accelerated diabetic wound healing, shown by a lower proportion of unhealed wounds (Fig. 2C) and reduced healing time (Fig. 2D) in the DM+Ins group compared to the DM group. Histological observations revealed rapid re-epithelialization (Fig. 2E,F) and extensive extracellular matrix deposition (Fig. 2G) in the DM+Ins group compared to the DM group. Many studies have revealed that macrophages are the orchestrators of wound healing, which is mediated by macrophage polarization from M1 to M2 states (Mantovani et al., 2013). The processes of re-epithelialization and extracellular matrix deposition are both intensively regulated by M2 macrophages. Thus, macrophage polarization from M1 to M2 and the resolution, that is, the further migration of M2 macrophages out into the wound, are the key steps of wound healing, marking the progression of healing from the inflammatory phase to the proliferation phase. We also observed the infiltration and resolution of macrophages on wound areas. We found significantly impaired macrophage infiltration and resolution in DM group wounds when compared with the Norm group wounds, which were characterized by less infiltration during the early stage of healing and delayed resolution at the late stage of healing. Insulin application ameliorated the abnormal macrophage infiltration and resolution of diabetic wounds (Fig. 2H,I). In DM+Ins group wounds, 4 days after wounding, there were many more infiltrating macrophages, whereas 12 days after wounding, these inflammatory cells began to withdraw from the wound area. Thus, based on the observation and comparison of wound healing time, unhealed wound proportion, rapid re-epithelialization and extensive extracellular

Journal of Cell Science (2020) 133, jcs235838. doi:10.1242/jcs.235838

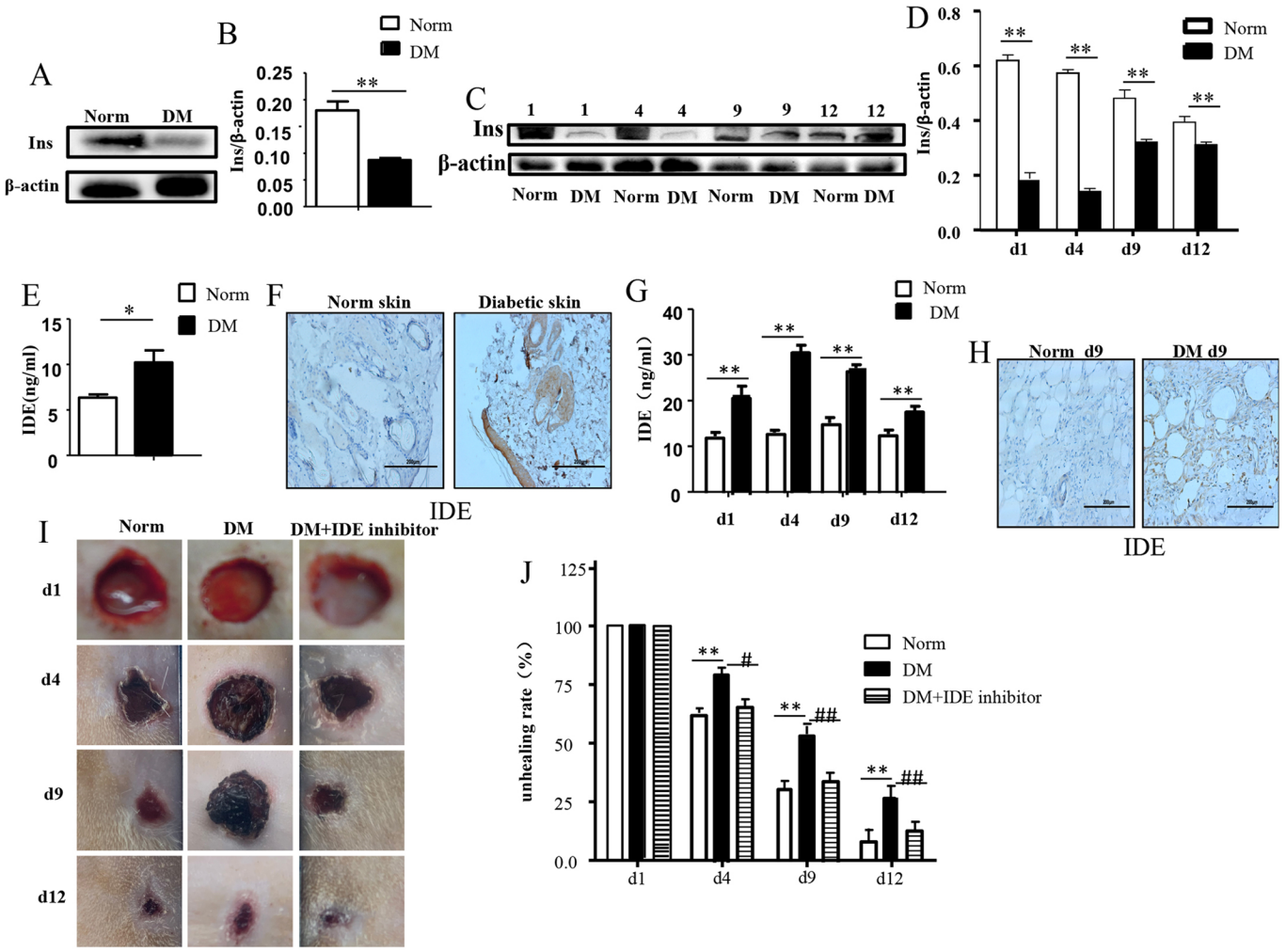

Fig. 1. Diabetic skin and diabetic wounds show a lower insulin level, which is possibly caused by overexpression of IDE in diabetic skin tissue. (A,B) Insulin (Ins) levels in the skin of normal (Norm) and diabetic (DM) rats were analyzed by western blotting and quantified relative to levels of β-actin. Data in B are mean±s.d. n=5. $^{**}P$<0.01. (C,D) Insulin levels in normal and diabetic wounds at 1, 4, 9 and 12 days after wounding (d1, d4, d9 and d12, respectively) were analyzed by western blotting and quantified relative to levels of β-actin. Data in D are mean±s.d. n=5. $^{**}P$<0.01. (E) To examine IDE expression in the diabetic state, dorsal skin from diabetic and normal rats was harvested and homogenized, and the supernatants were subject to ELISA examination. Data are mean±s.d. n=5. $^{*}P$<0.05. (F) *In situ* examination of IDE expression in normal and diabetic skin, as detected by immunohistochemistry. (G) To further examine the IDE expression level during wound healing, the wounds were harvested and homogenized, and the supernatants were subject to ELISA examination of IDE expression at different times of wound healing. Data are mean±s.d. n=5. $^{**}P$<0.01. (H) *In situ* examination of IDE expression in the wound by immunohistochemistry at day 9 after wounding. (I,J) The effect of IDE inhibition (DM+IDE inhibitor) on diabetic wound healing. All rats were photographed at the same height and show an area of an area of 13 mm × 13 mm. Wound sizes were recorded at 1, 4, 9 and 12 days after wounding using transparent tracing paper. The percentage of initial wound area remaining unhealed at each time was calculated using Image Pro Plus. Data are mean±s.d. n=3. $^{\#}P$<0.05; $^{**/\#\#}P$<0.01; *, Norm versus DM; #, DM versus DM+IDE inhibitor.

matrix deposition and resolution, we confirmed that, compared to the DM group, the application of topical insulin to diabetic wounds (DM+Ins group) significantly promoted the wound healing process, which ultimately enhanced the infiltration and resolution of macrophages around the wound area.

Insulin application regulates and promotes macrophage polarization from M1 to M2 phenotype in diabetic wounds

It is well known that macrophages are involved in manipulation of wound healing through their polarization and transition from M1 to M2 phenotype. M2 macrophages progress wounds towards the healing process, whereas M1 phenotype macrophages keep the wound in the chronic inflammation state (El Kebir and Filep, 2010; Mantovani et al., 2013). To investigate whether the infiltration and resolution of macrophages were results of the macrophage polarization transformation, we next investigated the macrophage polarization phenotype after insulin application. We observed an extensive and persistent pro-inflammatory M1 (iNOS-positive) macrophage phenotype in the DM group wounds at day 9 and day 12 after wounding. Insulin application considerably alleviated M1 macrophage accumulation (Fig. 3A,B). The number of cells positive for the M2 macrophage phenotype marker arginase 1 in the DM group was significantly lower than that in the Norm group at 9 and 12 days after wounding. M2 also became the major phenotype of macrophages in wounds at day 9 after wounding in the DM+Ins group, which suggested that the topical application of insulin in the wounds promoted macrophage polarization to the M2 phenotype (Fig. 3C,D). To further confirm this observation, we subsequently detected pro-inflammatory and anti-inflammatory mediators and markers in the wounds. Expression levels of the M1-macrophage-related pro-inflammatory mediators and markers IL-1β and iNOS (also known as NOS2) were significantly higher in the DM group wounds at day 9

Journal of Cell Science (2020) 133, jcs235838. doi:10.1242/jcs.235838

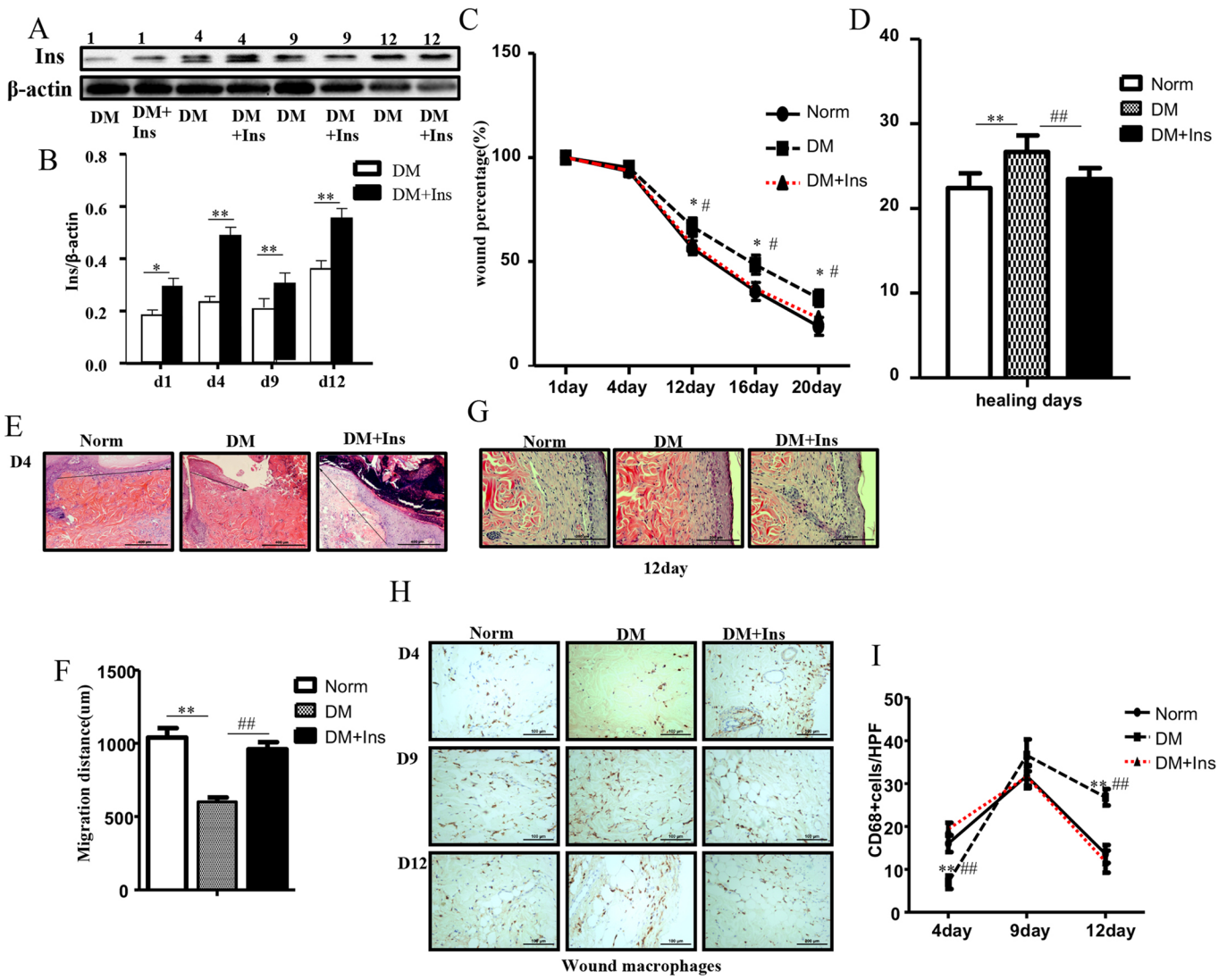

Fig. 2. Topical insulin supplement promotes diabetic wound healing and macrophage infiltration and resolution. (A,B) Insulin topical application elevates local insulin level in diabetic wounds. Insulin levels (Ins) at 1, 4, 9 and 12 d after wounding in DM and DM+Ins groups, analyzed by western blotting and quantified relative to levels of β-actin. Data are mean±s.d. *n*=5. (C,D) Wound sizes were recorded at 1, 4, 12, 16 and 20 days after wounding, using transparent tracing paper (C). The percentage of initial wound area remaining unhealed at each time was calculated using Image Pro Plus. The time taken for wounds to heal was also recorded (D). Data are presented as mean±s.d. *n*=5. (E–G) Wound re-epithelialization at 4 days after wounding (E,F) and extracellular matrix deposition at 12 days after wounding (G) for the three experimental groups. Arrows in E indicate the length of epithelial migration tongue. Data in F show epithelial migration distance and are presented as the mean±s.d. *n*=5. (H,I) Macrophage infiltration and resolution in the three experimental groups was assayed by CD68 staining at 4, 9 and 12 days after wounding. The number of CD68-positive cells per high-powered field of view (HPF) was calculated using Image Pro Plus. Data are shown as the mean±s.d. *n*=5. $^{*/\#}P<0.05$; $^{**/\#\#}P<0.01$; *, Norm versus DM; #, DM versus DM+Ins.

and day 12 after wounding, compared to levels in the Norm group. Insulin application significantly decreased IL-1β and iNOS levels and enhanced the expression of the M2-related cytokine IL-10 and the marker CD206 (also known as MRC1) in the DM+Ins group wounds (Fig. 3E–I). These results proved that insulin application simulated and promoted macrophage polarization and the change from M1 to M2 phenotype, and thus expedited the healing of diabetic wounds.

Insulin application promotes neutrophil infiltration and apoptosis

We have proven that topical insulin application can stimulate an improved macrophage reaction in diabetic wounds. Because cytokines are the main substance secreted during hemostasis and the inflammatory phase of healing, we performed cytokine array analysis to comprehensively understand the influence of insulin application on macrophage responses and the inflammatory reaction (Fig. 4A). We set the level of cytokines in the normal wound group 1 day after wounding as a control/base number and the relative expression levels in the other groups were calculated (Fig. 4B). The relative expression rate is defined as the ratio of the expression level of a given cytokine in the sample of interest and the level of the same cytokine in the Norm group wounds 1 day after wounding. The protein arrays further confirmed that the macrophage polarization from M1 to M2 phenotype was severely impaired in the DM group. The levels of M1-phenotype-related markers or related pro-inflammation cytokines such as CD86, IL-1β, CNTF and IL-6 were higher in the DM group wounds at day 9, and even at day 12 after wounding (Fig. 4C). At the same time, the expression of M2-related markers and related cytokines or growth factors such as IL-4, IL-10, PDGF and TIMP-1 were lower in the diabetic group wounds

Journal of Cell Science (2020) 133, jcs235838. doi:10.1242/jcs.235838

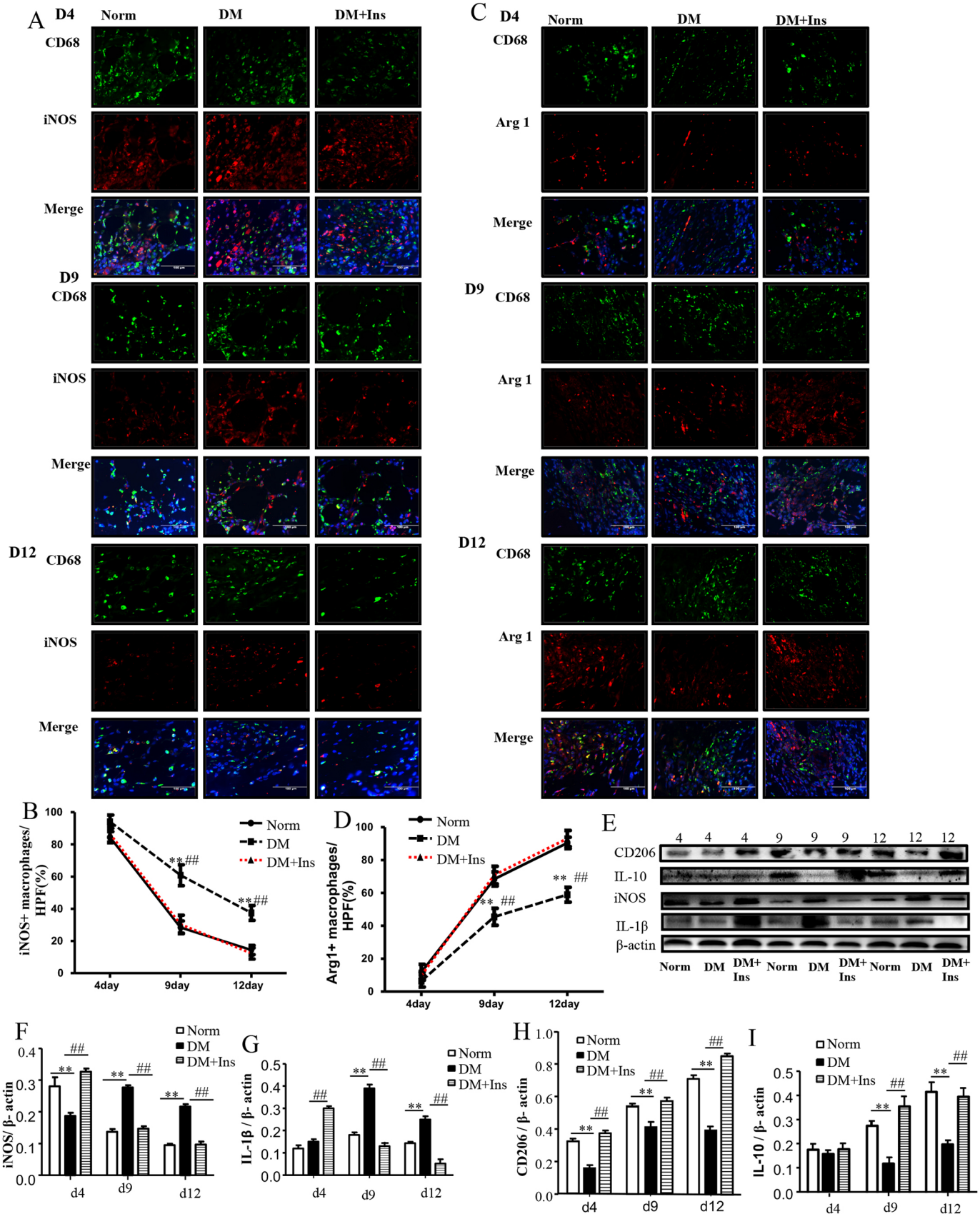

Fig. 3. See next page for legend.

Journal of Cell Science (2020) 133, jcs235838. doi:10.1242/jcs.235838

Fig. 3. Insulin application promotes macrophage phenotype polarization in diabetic wounds. (A,B) M1 macrophage tendency was analyzed by immunofluorescence at 4, 9 and 12 days after wounding (D4, D9 and D12, respectively). CD68 was used as a marker of total macrophages and iNOS was used as a pro-inflammation marker. Double fluorescence-positive cells were identified as M1 macrophages. Green, CD68; red, iNOS; blue, DAPI. The M1 macrophages were identified and analyzed by Image Pro Plus, and the percentage of total macrophages identified as M1 macrophages in each high-powered field of view (HPF) was calculated for the different groups at different times after wounding. Data are shown as the mean±s.d. n=5. (C,D) M2 macrophage tendency at 4, 9 and 12 days after wounding. CD68 was used as a marker of total macrophages and arginase 1 (Arg 1) was used as a pro-healing marker. Double fluorescence-positive cells were identified as M2 macrophages. Green, CD68; red, arginase1; blue, DAPI. The M2 macrophages were identified and analyzed by Image Pro Plus, and the percentage of total macrophages identified as M2 macrophages in each high-powered field of view (HPF) was calculated for the different groups at different times after wounding. Data are shown as the mean±s.d. n=5. (E–I) iNOS and IL-1β were regarded as markers of M1 macrophages, whereas arginase 1 and CD206 were taken as markers of M2 macrophages. Western blotting was used to examine M1 and M2 macrophage-related marker expression tendency at 4, 9 and 12 days after wounding in the three experimental groups. β-actin was used as a loading control. Expression of each marker was quantified relative to β-actin expression. Data are shown as the mean±s.d. n=5. $^{*/\#}P<0.05$; $^{**/\#\#}P<0.01$; *, Norm versus DM; #, DM versus DM+Ins.

when compared with the Norm group wounds. Insulin application reversed these abnormalities, and the DM+Ins group wounds showed decreased expression of M1-related cytokines and increased expression of M2-related markers (Fig. 4C,D). These observations confirmed that insulin application promoted the macrophage polarizing phenotype change from M1 to M2, which is impaired in the diabetic wound environment. Furthermore, we found that cytokines related to neutrophil chemotaxis, survival and apoptosis were also actively regulated by the insulin application. Chemokines that function to recruit and activate neutrophils, such as thymus chemokine-1, CINC-1 (also known as CXCL1), CINC-2 (CXCL3) and CINC-3 (CXCL2), were relatively lower in the DM group wounds 1 day after wounding when compared with levels in the Norm group wounds. Insulin application to the DM+Ins group increased the expression of these chemokines to levels that were very close to those in the Norm group. The expression of thymus chemokine-1, CINC-1, CINC-2 and CINC-3 were significantly decreased on day 9 and day 12 after wounding in the Norm group wounds, whereas in diabetic wounds these chemokines were still at relatively high expression levels. The expression pattern of these chemokines revealed that, in diabetic wounds, neutrophil infiltration and resolution were impaired and that, even in the late stage of the inflammatory phase, large amounts of neutrophils still existed in the wounds. It is worth noting that consistent neutrophil infiltration is commonly seen in most chronic wounds. In insulin-treated wounds, the expression pattern of neutrophil chemokines was similar to the expression in normal wounds (Fig. 4E), which suggested that topical insulin application alleviated impaired neutrophil infiltration and resolution. The expression levels of cytokines related to the survival and apoptosis of neutrophils, namely GM-CSF (CSF2), Fas-ligand (FASLG) and TNF-α, and of the neutrophil-specific proteinase MMP-8, also confirmed this finding (Fig. 4F). To further validate that insulin application improved neutrophil infiltration and resolution, we checked neutrophil infiltration and resolution using Hematoxylin and Eosin (H&E), IHC and TUNEL staining. H&E combined with IHC staining showed delayed neutrophil infiltration at the early stage of healing and impaired resolution at the late stage in the DM group wounds (Fig. 4G–I). TUNEL analysis was applied to check the status of neutrophil apoptosis. Neutrophil apoptosis was detected using TUNEL and neutrophil marker CD66b double staining. Compared with the Norm group wounds, fewer apoptotic neutrophils were found in DM group wounds at day 4 after wounding. Insulin application significantly increased apoptotic neutrophil numbers in the area of DM+Ins group wounds (Fig. 4J,K). Accelerating inflammatory cell infiltration and resolution in diabetic wounds following insulin application suggested that topical insulin application reversed the impaired diabetic inflammatory response.

Apoptosed neutrophils further positively regulate and promote macrophage polarization from M1 to M2 phenotype

To determine whether insulin could directly regulate inflammatory cell function, we detected the expression of insulin receptor (IR) and insulin-like growth factor receptor 1 (IGFR1). These are the main receptors that are involved in the insulin signaling pathway in neutrophils and macrophages. We detected positive IR and IGFR expression in both peritoneal neutrophils and macrophages (Fig. 5A,B). Meanwhile, we also observed positive IR and IGFR expression in wound neutrophils and macrophages (Fig. 5C,D), which suggested that insulin could regulate inflammatory cell function in an IR- or IGFR-dependent manner.

Neutrophils are the first nucleated cells to infiltrate the wound after wounding. Recent studies reported that apoptosed neutrophils can induce macrophage phenotype transition, and that this transition is regarded as the initiator of macrophage phenotype switching from M1 to M2 (El Kebir and Filep, 2010; El Kebir and Filep, 2013; Wilgus et al., 2013). This raises the possibility that the insulin-application-induced improvement of macrophage phenotype polarization is correlated with enhanced neutrophil apoptosis in the diabetic wound environment. We next investigated the effects of apoptosed neutrophils on the macrophage phenotype transition. We isolated neutrophils and macrophages from the rat peritoneal cavity. In an *in vitro* study, we used apoptosed neutrophils to stimulate M1 macrophages, and checked effect of the apoptosed neutrophils on macrophage polarization. After efferocytosis of apoptosed neutrophils, macrophages initiated polarization, switching from M1 to M2 phenotype. Increased expression of CD206 and IL-10 and reduced expression of iNOS were detected in the apoptotic group by western blotting (Fig. 5E–H). Immunofluorescence staining also confirmed this phenotype transformation of macrophages, as shown by downregulation of expression of M1-related markers and upregulated expression of M2-related markers (Fig. 5I–L). Taken together, these results confirmed that the apoptosed neutrophils could promote macrophage polarization and the transition from M1 to M2 phenotype.

Based on these results, we further studied whether the promoting function of insulin on the macrophage phenotype transformation from M1 to M2 was mediated by the promotion of neutrophil apoptosis. Neutrophil apoptosis during wound healing is mainly induced by phagocytosis (the process of phagocytosis-induced apoptosis). We next investigated the effect of insulin on neutrophil phagocytosis function and the process of phagocytosis-induced apoptosis. We found that the phagocytosis of diabetic-derived neutrophils was significantly damaged. Among the experimental groups, the fewest engulfed FITC-labeled *E. coli* were observed in the diabetic neutrophils. An obviously enhanced phagocytosis function was observed for diabetic neutrophils in the presence of insulin, which suggested that insulin promoted neutrophil phagocytosis function (Fig. 5M). We next investigated the phagocytosis-induced apoptosis of neutrophils after engulfing heat-killed *E. coli*. After incubation, apoptosis of neutrophils was

Journal of Cell Science (2020) 133, jcs235838. doi:10.1242/jcs.235838

A

	A	B	C	D	E	F	G	H	I	J	K	L
1	POS1	POS2	POS3	NEG	Activin A	Agrin	B7-2 / CD86	β-NGF	CINC1	CINC2a	CINC3	CNTF
2	POS1	POS2	POS3	NEG	Activin A	Agrin	B7-2 / CD86	β-NGF	CINC1	CINC2a	CINC3	CNTF
3	FASLG	CX3CL1	CSF2	ICAM1	IFN-γ	IL-1α	IL-1β	IL1 R6	IL-2	IL-4	IL-6	IL-10
4	FASLG	CX3CL1	CSF2	ICAM1	IFN-γ	IL-1α	IL-1β	IL1 R6	IL-2	IL-4	IL-6	IL-10
5	IL-13	Leptin	LIX	SELL	MCP1	MIP-3α	MMP-8	PDGF-AA	PRLR	RAGE	CXCL7	TIMP1
6	IL-13	Leptin	LIX	SELL	MCP1	MIP-3α	MMP-8	PDGF-AA	PRLR	RAGE	CXCL7	TIMP1
7	TNF-α	VEGF-A	NEG	NEG	NEG	NEG	NEG	NEG	NEG	NEG	NEG	POS4
8	TNF-α	VEGF-A	NEG	NEG	NEG	NEG	NEG	NEG	NEG	NEG	NEG	POS4

B

	N1	D 1	INS1	N4	D4	INS4	N9	D9	INS9	N12	D12	INS12
Activin	1	0.69	0.93	2.19	1.62	2.38	1.31	0.97	1.6	0.31	0.57	0.47
Agrin	1	0.5	1.04	0.94	0.21	0.68	0.3	0.29	0.24	0.17	0.51	0.21
B7-2/CD	1	0.8	1.16	2.97	1.89	3.26	1.44	2.74	1.55	0.62	1.8	0.73
beta-NG	1	1.17	1.06	1.44	3.07	1.82	0.29	2.8	0.38	0.19	2.08	0.42
CINC-1	1	0.39	0.9	1.07	1.74	0.91	0.43	1.63	0.36	0.16	0.67	0.25
CINC-2	1	0.54	0.95	2.71	5.7	3.05	0.26	4.74	0.34	0.23	3.2	0.38
CINC-3	1	0.49	0.99	0.59	0.73	0.66	0.35	0.71	0.36	0.31	0.29	0.22
CNTF	1	0.41	0.66	1.06	0.94	0.93	0.15	1.32	0.28	0.32	0.72	0.2
Fas Lig	1	0.6	1.05	1.18	0.63	1.12	0.67	1.1	0.46	0.34	1.12	0.47
Fractal	1	0.48	1.04	0.71	0.75	0.68	0.47	1.59	0.39	0.27	1.69	0.39
GM-CSF	1	0.64	1.52	1.01	0.85	0.98	0.13	0.94	0.18	0.18	0.22	0.13
ICAM-1	1	0.49	1.46	1.76	2.12	1.59	0.55	1.38	0.5	0.43	0.87	0.31
IFN-gam	1	1.21	0.99	2.36	6.73	1.92	1.08	3.23	1.32	1.03	2.13	1.22
IL-1 al	1	0.37	1.07	1.19	1.18	1.24	0.38	0.97	0.28	0.13	1.04	0.1
IL-1 be	1	0.62	0.97	1.88	1.11	1.73	0.4	1.5	0.48	0.18	1.22	0.27
IL-1 R6	1	0.48	1	1.04	1.16	1.05	0.88	1.23	0.94	0.33	0.66	0.28
IL-2	1	0.36	1.09	0.74	0.82	0.87	0.43	1.33	0.31	0.14	0.48	0.25
IL-4	1	0.3	1.07	1.61	0.78	1.43	1.91	0.96	1.85	3.1	1.65	2.8
IL-6	1	0.38	1.15	1	1.03	1	0.5	1.38	0.66	0.22	0.36	0.32
IL-10	1	0.17	1.12	1.35	1.1	1.48	2.06	1.31	2.41	2.32	1.44	2.69
IL-13	1	0.57	1.06	1.43	1.81	2.16	0.21	0.87	0.27	0.26	0.69	0.34
Leptin	1	0.86	0.9	3.91	3.66	3.25	1.29	3.16	1.11	0.47	0.98	0.52
LIX	1	0.52	1.17	1.15	0.95	1.1	0.56	1.54	0.48	0.38	1.32	0.54
L-Selec	1	1.12	0.98	0.56	0.81	0.47	0.48	1.48	0.32	0.23	0.63	0.36
MCP-1	1	0.45	1.12	7.87	3.15	6.3	1.29	4	1.55	0.37	0.74	0.22
MIP-3 a	1	0.09	1.02	1.29	1.63	1.47	0.4	0.97	0.52	0.32	0.79	0.26
MMP-8	1	0.28	0.97	0.35	0.75	0.46	0.28	0.67	0.22	0.1	0.41	0.13
PDGF-AA	1	0.57	1.11	0.72	0.41	0.89	1.41	0.58	1.23	0.69	0.81	0.74
Prolact	1	0.14	0.85	0.91	0.63	0.78	0.42	0.82	0.53	0.21	0.97	0.53
RAGE	1	1.29	0.95	1.8	1.94	1.15	1.04	1.62	1.17	1.05	1.5	0.98
Thymus	1	0.23	1.06	1.46	2.33	1.41	0.9	1.89	0.74	0.47	1.36	0.25
TIMP-1	1	0.33	1.37	2.31	0.91	1.9	2.72	1.49	2.48	2.57	2.1	2.63
TNF-alp	1	0.52	1.08	2.17	1.18	2	0.31	1.43	0.28	0.13	1.1	0.1
VEGF	1	0.54	0.91	15.8	9.54	14.7	3.87	3.69	4.18	0.56	0.64	0.54

C

	N1 vs D 1	INS 1 vs D 1	N 4 vs D 4	INS 4 vs D4	N 9 vs D 9	INS 9vs D 9	N12 vs D 12	INS 12 vs D 12
CD86			↑↑	↑↑	↓↓	↓↓	↓↓	↓↓
CNTF	↑↑	↑↑			↓↓	↓↓	↓↓	↓↓
IL-1 α	↑↑	↑↑			↓↓	↓↓	↓↓	↓↓
IL-1 β	↑↑	↑↑	↑↑	↑↑	↓↓	↓↓	↓↓	↓↓
IL-1 R6	↑↑	↑↑					↓↓	↓↓
IL-2	↑↑	↑↑			↓↓	↓↓	↓↓	↓↓
IL-13	↑↑	↑↑			↓↓	↓↓	↓↓	↓↓
IL-6	↑↑	↑↑			↓↓	↓↓	↓↓	

D

	N1 vs D 1	INS 1 vs D 1	N 4 vs D 4	INS 4 vs D 4	N 9 vs D 9	INS 9vs D 9	N12 vs D 12	INS 12 vs D 12
IL-10	↑↑	↑↑			↑↑	↑↑	↑↑	↑↑
IL-4	↑↑	↑↑	↑↑	↑↑	↑↑	↑↑	↑↑	↑↑
TIMP-1	↑↑	↑↑	↑↑	↑↑	↑↑	↑↑		
PDGF	↑↑	↑↑	↑↑	↑↑	↑↑	↑↑		
VEGF	↑↑	↑↑	↑↑	↑↑				

E

	N1 vs D 1	INS 1 vs D 1	N 4 vs D 4	INS 4 vs D 4	N 9 vs D 9	INS 9vs D 9	N12 vs D 12	INS 12 vs D 12
CINC1	↑↑	↑↑	↓↓	↓↓	↓↓	↓↓	↓↓	↓↓
CINC2	↑↑	↑↑	↓↓	↓↓	↓↓	↓↓	↓↓	↓↓
CINC3	↑↑	↑↑			↓↓	↓↓		
CXCL7	↑↑	↑↑	↓↓	↓↓	↓↓	↓↓	↓↓	↓↓
LIX	↑↑	↑↑			↓↓	↓↓	↓↓	↓↓
ICAM1	↑↑	↑↑			↓↓	↓↓	↓↓	↓↓

F

	N1 vs D 1	INS 1 vs D 1	N 4 vs D 4	IN 4 vs D 4	N 9 vs D 9	INS 9vs D 9	N12 vs D 12	INS 12 vs D 12
Fas Ligand	↑↑	↑↑	↑↑	↑↑	↓↓	↓↓	↓↓	↓↓
GM-CSF	↑↑	↑↑			↓↓	↓↓		
TNF-α	↑↑	↑↑	↑↑	↑↑	↓↓	↓↓	↓↓	↓↓
MMP-8	↑↑	↑↑	↓↓	↓↓	↓↓	↓↓	↓↓	↓↓

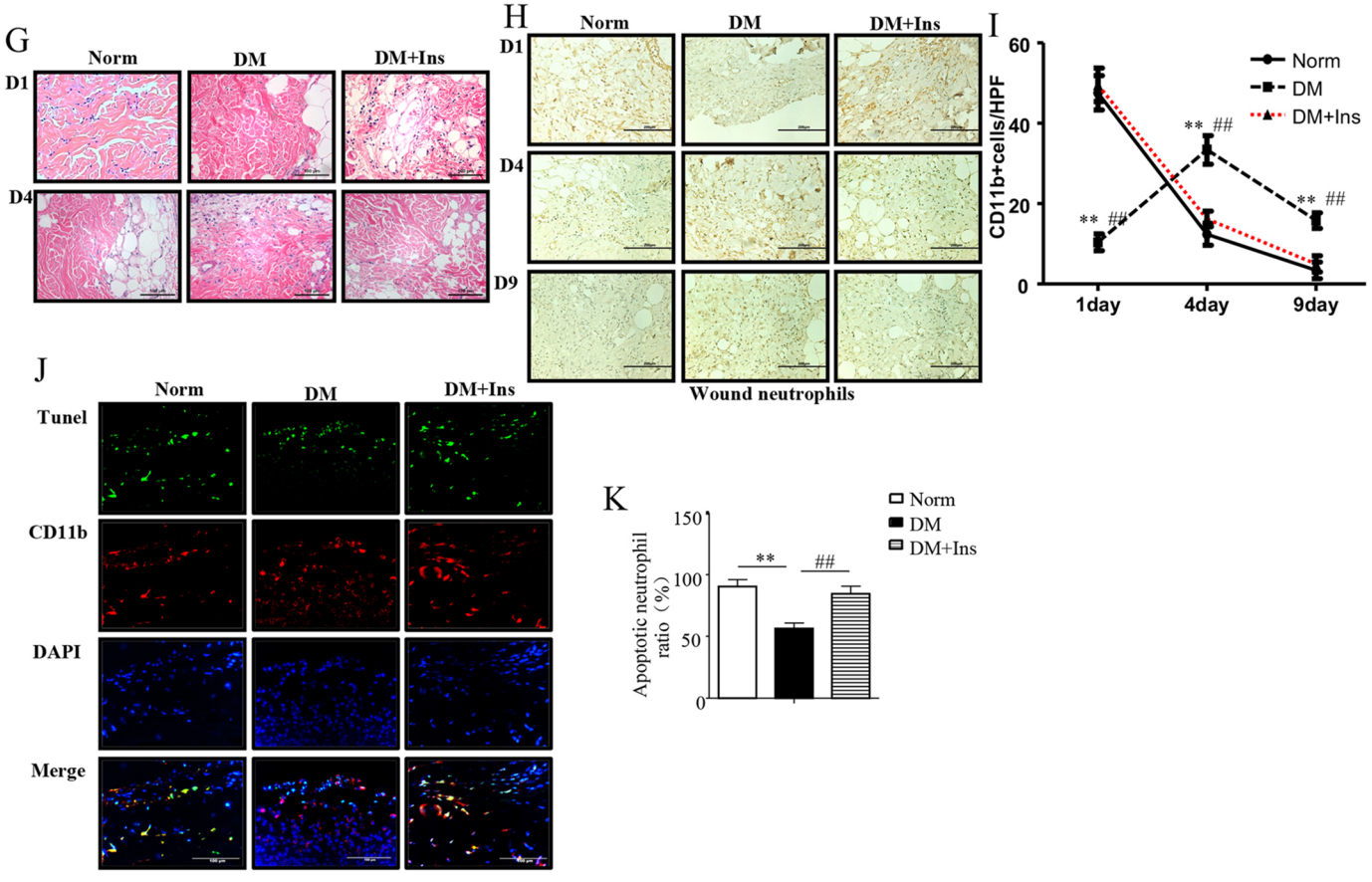

Fig. 4. See next page for legend.

Journal of Cell Science (2020) 133, jcs235838. doi:10.1242/jcs.235838

Fig. 4. Insulin application promotes neutrophil infiltration and apoptosis. (A) The layout of the cytokine array. (B) The fluorescence intensities recorded in the cytokine array assay were normalized to values measured for the normal group at 1 day after wounding (N1). Relative expression values for samples from diabetic wounds (D) and insulin-treated diabetic wounds (INS) at 1, 4, 9 and 12 days after wounding are shown. Red indicates downregulated, and green indicates upregulated when compared with the separate relative expression at N1. (C) M1 and pro-inflammation cytokine markers and cytokine expression at 1, 4, 9 and 12 days after wounding was analyzed and compared between experimental groups (normal, N; diabetic, D; insulin-treated, INS). ↑↑ indicates significant upregulation, ↓↓ indicates significant downregulation. n=3. (D) Comparison of M2-related cytokines and growth factor expression between the experimental groups at different times after wounding, as described in C. (E) Expression of cytokines related to neutrophil attraction, migration and molecular adhesion was compared between experimental groups at different times after wounding. The data are shown as described in C. (F) Neutrophil survival- and apoptosis-related cytokine expression was compared between experimental groups at different times after wounding. The data are shown as described in C. (G–I) Neutrophil infiltration and resolution in the three experimental groups, as labeled by Hematoxylin and Eosin staining at 1 and 4 days after wounding (G), and by CD11b staining at 1, 4 and 9 days after wounding (H). The proportion of CD11b-positive cells per high-powered field of view (HPF) was calculated using Image Pro Plus (I). Data are mean±s.d. n=5. (J,K) Neutrophil apoptosis at 4 days after wounding was analyzed by a TUNEL assay combined with immunofluorescence. CD11b was used as a marker of neutrophils. Green, TUNEL; red, CD11b; blue, DAPI. The apoptosis rates of neutrophils were calculated using Image Pro Plus. Data are the mean±s.d. n=5. $^{**/\#\#}P$<0.01; *, Norm versus DM; #, DM versus DM+Ins.

measured by analysis of caspase 3 expression. Significantly lower expression of cleaved caspase 3 was observed in diabetic neutrophils compared to levels in the Norm group. Insulin application promoted expression of cleaved caspase 3 and further apoptosis (Fig. 5N,O). Macrophage efferocytosis, the process of phagocytosis of apoptotic neutrophils by macrophages, induces macrophages to switch from M1 to M2 phenotype (Ortega-Gómez et al., 2013). Next, we studied macrophage efferocytosis function. We found significantly impaired efferocytosis by diabetic peritoneal macrophages compared to that by macrophages from the peritoneal cavity of normal rats. Insulin treatment also significantly increased efferocytosis by diabetic macrophages (Fig. 5P).

All these results showed that insulin application could normalize the impaired functions of neutrophils and macrophages in diabetic wounds, induce a balanced inflammation reaction and promote wound healing.

DISCUSSION

Many studies have revealed that blood normalization by insulin can improve the neutrophil dysfunctions of diabetes patients. Some have attributed the recovery of neutrophil function to improved control of blood glucose, whereas others discovered that the insulin-promoted neutrophil function is independent of glucose normalization and could be attributed to the direct effects of insulin application on neutrophil function (Lecube et al., 2011; Walrand et al., 2004). In this research, we found a deficiency of insulin in both uninjured diabetic skin tissue and diabetic wounds, as compared to the levels in non-diabetic wounds, even though the serum insulin level of the diabetic group was relatively higher than the non-diabetic group. In conjunction with the low insulin expression, high IDE expression was detected in diabetic skin and diabetic wounds. IDE is supposed to be expressed in all tissues, including the skin, and it exists in many subcellular compartments and the extracellular milieu. In the diabetic state, many factors may contribute to the high expression of IDE, including high plasma glucose, high levels of free fatty acids (FFA), and the presence of pro-inflammatory cytokines, such as IL-6 (Tang, 2016). In our study, we found a consistently high level of IDE expression in diabetic wounds, and observed that IDE level in diabetic wounds decreased as healing progressed, which was similar to the changes in levels of pro-inflammatory cytokines. As for insulin expression, in early stages of non-diabetic wound healing, the high level of insulin in the wound area may come from plasma, due to increased blood vessel permeability during the inflammatory response. As healing is achieved, vascular endothelial cells undergo apoptosis, and wound blood vessel occlusion occurs, and insulin levels decrease correspondingly. In diabetic wound healing, however, a higher IDE level in early stages of healing would degrade wound insulin and lead to low insulin expression. Meanwhile, delayed diabetic wound healing could induce a delayed and persistent insulin accumulation in wounds. Our results suggest that excessive IDE activity leads to a lower insulin level in diabetic wounds, which provides the possibility of accelerating wound healing by topical insulin application.

The presence of IR and IGFR in neutrophils and macrophages raises the possibility that insulin directly regulates the functions of diabetic neutrophils and macrophages. We used various approaches, including H&E and IHC staining, immunofluorescence staining and cytokine array analysis, to investigate the diabetic wound inflammatory response. All results demonstrated the delayed but consistent infiltration of neutrophils in diabetic wounds, which is a typical feature of chronic inflammation (Pierce, 2001; Nunan et al., 2014; Allen et al., 2007). *In vitro* studies revealed an impaired phagocytosis function of neutrophils. Delightfully, the impaired neutrophil function was rectified by insulin application. Besides neutrophils, impaired macrophage function, specifically impaired phenotype transition, was also noticed in diabetic wounds. It is known that apoptotic neutrophils are capable of inducing macrophage phenotype transition. To explore apoptosis of diabetic neutrophils, we measured neutrophil apoptosis-related mediators. As reported previously, TNF-α regulates neutrophil apoptosis in a bi-directional manner, which means that TNF-α could promote the apoptosis of neutrophils when present at a high level and promote the survival of neutrophils when present at a moderate or low level (Luo and Loison, 2008). Protein arrays showed that the TNF-α level in the diabetic wound was persistent at a medium level, whereas the normal group and the insulin-application group had an expression peak in the 4th day after wounding. Consistent with the TNF-α expression peak in the normal group and insulin-application group, a high rate of neutrophil apoptosis was found in both groups. The Fas-ligand and GM-CSF analysis also revealed that the neutrophils tended to survive in the diabetic wound environment (Martin et al., 2015). The prolonged survival of neutrophils might disrupt macrophage polarization, due to a lack of sufficient stimuli that trigger macrophage polarization (Mantovani et al., 2013). The expression levels of macrophage-polarization-related cytokines also confirmed these discoveries. We found that expression of the M1-related cytokines was relatively higher, whereas the expression of M2-related cytokines was persistently lower in the diabetic group, compared to levels in the Norm group. Insulin supplement may normalize the impaired migration and phagocytosis function of neutrophils. Phagocytosis-induced apoptosis was also confirmed by *in vitro* examination. By engulfing the apoptosed neutrophils, macrophages initiate the polarization phenotype transition from M1 to M2 and promote the resolution of inflammation at the wound (Poon et al., 2014). One flaw of our study is that we did not exclude the possibility of insulin directly affecting the macrophage phenotype transformation; however, to the best of our knowledge, the apoptosis of neutrophils is the more crucial factor in triggering macrophage polarization during wound healing. We have used

Journal of Cell Science (2020) 133, jcs235838. doi:10.1242/jcs.235838

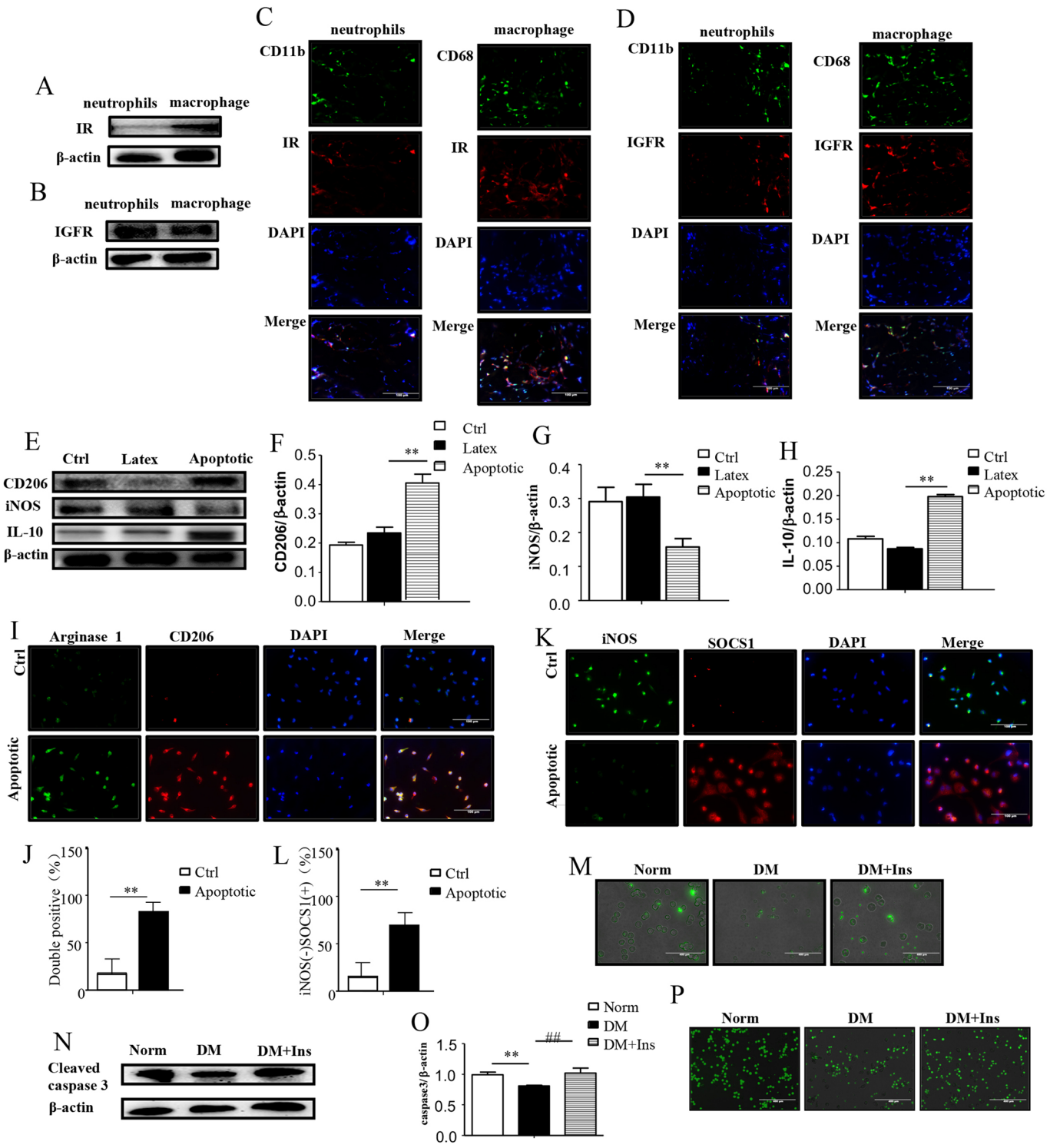

Fig. 5. See next page for legend.

BALB/c mice (note, because there were no neutrophil-neutralizing antibodies for rats, BALB/c mice were used to observe the effect of neutrophil depletion on macrophage polarization in wounded skin tissues) to observe the direct effect of neutrophils on macrophage polarization in wounded skin tissues (Fig. S1A–D). We found that neutrophil depletion could impair macrophage polarization and transition from M1 to M2 during wound healing, and this result was consistent with the work of other scientists (El Kebir and Filep, 2010; El Kebir and Filep, 2013; Wilgus et al., 2013). Taken together, our studies have revealed that the application of extra insulin could normalize the wound insulin level locally, restore neutrophil and macrophage function in the wound and ultimately promote diabetic wound healing.

In addition to the above conclusions, there are still some considerations that need to be discussed. Firstly, in the diabetic state, some impairments of the insulin signaling pathway in neutrophils

Journal of Cell Science (2020) 133, jcs235838. doi:10.1242/jcs.235838

Fig. 5. Apoptosed neutrophils promote transition of macrophage polarization phenotype from M1 to M2. (A,B) Western blot analysis of IR and IGFR expression in neutrophils and macrophages. β-actin is shown as a loading control. (C) Fluorescence double staining was used in the examination of IR expression in wound neutrophils and macrophages. CD11b is a marker of neutrophils. CD68 is a marker of macrophages. Red, IR; green: neutrophils marker CD11b, or macrophage marker CD68; blue, DAPI. (D) Fluorescence double staining was also used to examine IGFR expression in wound neutrophils and macrophages. Red, IGFR; green: neutrophil marker CD11b or macrophage marker CD68; blue, DAPI. (E–H) Macrophages were lysed 24 h after treatment with apoptosed neutrophils, and the expression of CD206, iNOS and IL-10 was analyzed by western blotting (Ctrl, control; Latex, latex-bead-treated sample). β-actin is shown as a loading control. Data in F–H show the mean±s.d. expression relative to β-actin. n=3. $^{**}P$<0.01. (I–L) Wound macrophages were either treated with apoptosed neutrophils for 24 h (Apoptotic) or left untreated (Ctrl) before being fixed and subjected to double immunofluorescence staining to analyze the macrophage phenotype transformation. Arginase 1, CD206 and SOCS1 were used as M2 macrophage markers and iNOS was used as an M1 macrophage marker. Green, arginase 1 (I), iNOS (K); red, CD206 (I), SOCS1(K); blue, DAPI. The proportion of arginase 1 and CD206 double-positive cells was scored (J), along with the proportion of iNOS-negative and SOCS1-positive cells (L). Data are shown as the mean±s.d. n=3. $^{**}P$<0.01. (M) Insulin improves the impaired phagocytosis function of neutrophils from diabetic wounds. Neutrophils isolated from diabetic peritoneal wounds were treated (DM+Ins) or untreated (DM) with 100 nM insulin for 1 h before FITC-labeled *E. coli* were added at a ratio of 10:1 (*E. coli*: neutrophils). Neutrophils from the normal peritoneal wounds were used as a positive control (Norm). After 60 min the cells were subject to fluorescence microscopy to analyze the phagocytosis of *E. coli*. (N,O) Neutrophils from peritoneal wounds were prepared, insulin treated and seeded with FITC-labeled *E. coli* as described for M. After 18 h, the cells were lysed and subjected to western blot analysis to detect cleaved caspase 3, in order to evaluate phagocytosis-induced apoptosis. β-actin is shown as a loading control. Data are presented as the mean±s.d expression relative to β-actin. n=3. $^{**/\#\#}P$<0.01; *, Norm versus DM; #, DM versus DM+Ins. (P) Neutrophils isolated from peritoneal wounds were labeled with CellTracker Green and cultured for 24 h to induce apoptosis. After the neutrophils were apoptosed, the apoptosed neutrophils were seeded on macrophages isolated from peritoneal wounds of normal and diabetic rats at a ratio of 4:1 (apoptosed neutrophils: macrophages). The diabetic macrophages were either untreated (DM) or pre-treated 100 nM insulin (DM+Ins). Macrophage efferocytosis of apoptosed neutrophils was analyzed by fluorescence microscopy 4 h after the addition of apoptosed neutrophils.

and macrophages do exist. However, many studies have reported that insulin can promote the function of neutrophils and macrophages in diabetes. For example, insulin can promote the phagocytosis and killing of neutrophils, and can also promote the expression of scavenger receptor in macrophages of diabetic rodents, thus enhancing their phagocytic function (Walrand et al., 2004, Alba-Loureiro et al., 2006). We argue that the damage of neutrophil and macrophage function in diabetes is caused by many mechanisms. Insulin level is one of them. Other mechanisms, such as high glucose level, accumulation of advanced glycation end products (AGEs) and oxidative stress, can also lead to damage of neutrophil and macrophage function (Berbudi et al., 2020; Baltzis et al., 2014; Frydrych et al., 2018; Forbes and Cooper, 2013). These circumstances could explain the results in Fig. 5M and P that showed reduced activity of neutrophils and macrophages isolated from diabetic rats compared to those from normal rats that were not treated with insulin. This research focused on situations where the high level of insulin-degrading enzyme in diabetic wounds degrades insulin, which leads to the wound insulin-insufficient state. Neutrophils and macrophages in the wound lack sufficient insulin to activate their functions, and insulin supplementation could improve the function of neutrophils and macrophages, and promote diabetic wound healing. Secondly, we did not examine the exact downstream signaling pathway by which insulin affects neutrophil and macrophage function. According to our previous work, and that of other researchers, insulin may regulate neutrophil activity through activation of PI3K–Akt, SPAK/JNK and p38 MAPK signaling pathways when binding to IR or IGFR, and downstream targets have been related to increased neutrophil functions, including chemotaxis, phagocytosis and bactericidal activity (Liu et al., 2018; Yano et al., 2012; Oldenborg and Sehlin, 1998).

MATERIALS AND METHODS

Reagents

Streptozocin (STZ) and thioglycolate were from Sigma-Aldrich (St Louis, MO), 60% high-fat diet was from Research Diets (New Brunswick, NJ), insulin was purchased from Lilly USA (LLC, Indianapolis), insulin for cell culture and TUNEL assay kit were obtained from Roche (Basel, Switzerland), DAPI (Life Technologies, Carlsbad, CA), FITC-labeled *E.coli* and CellTracker Green were purchased from ThermoFisher (Carlsbad, CA), RPMI 1640, DMEM and PBS were obtained from GIBCO (Carlsbad, CA), OCT compound was from Sakura Finetek (Torrance, CA), sandwich ELISA rat cytokine array G2 analysis was from Ray Biotech (Norcross, GA), arginase was from Cell Signaling Technology (Danvers, MA), chemiluminescence kit was from Millipore (Billerica, Massachusetts), insulin-degrading enzyme (IDE) inhibitor 6bK was from R&D Systems (Minnneapolis, MN).

The following antibodies were used: anti-iNOS at dilution: 1:50 for immunofluorescence of cells (IF), 1:1000 for western blotting (WB) (Life Technologies, Carlsbad, CA; catalog number PA1-036); anti-insulin receptor at dilution 1:100 for IF, 1:1000 for WB (catalog number ab5500), anti-IGF at dilution 1:1000 for WB (catalog number ab36532), anti-IGF receptor at dilution 1:50 for IF, 1:1000 for WB (catalog number ab182408), anti-IL-1β at dilution 1:1000 for WB (catalog number ab9722), anti-IDE at dilution 1:100 for IHC (catalog number ab32216) and anti-SOCS-1 at dilution 1:100 for IF (catalog number ab9870) were from Abcam (Cambridge Science Park, Cambridge); anti-insulin at dilution 1:1000 for WB (catalog number 4590S), anti-cleaved caspase-3 at dilution 1:1000 for WB (catalog number 9661S), anti-β-actin at dilution 1:1000 for WB, HRP-labeled secondary antibodies at dilution 1:1000 for WB (catalog numbers 7074S and 7076S; Cell Signaling Technology, Danvers, MA); anti-CD206 at dilution 1:50 for IF, 1:1000 WB (catalog number sc-376232) and anti-IL-10 at dilution 1:1000 for WB (catalog number sc-365858; Santa Cruz Biotechnology, Santa Cruz, CA); anti-CD11b at dilution 1:50 for IF and IHC (ABclonal Biotech, Woburn, MA; catalog number A1581); anti-CD68 at dilution 1:100 for IF and IHC, 1:1000 for WB (Bio-Rad, Philadelphia, PA; catalog number MCA5709); donkey anti-rabbit AlexaFluor-488 (catalog number R37118), donkey anti-mouse AlexaFluor-488 (catalog number R37114), donkey anti-mouse AlexaFluor-594 (catalog number A-21203), and donkey anti-rabbit AlexaFluor-594 (catalog number A21207); all the fluorescent second antibodies were diluted at 1:1000 for IF and IHC and were purchased from ThermoFisher (Carlsbad, CA).

Animals

90 male Wistar rats, 6 weeks old, weighing ∼120–140 g were purchased from Shanghai Laboratory Animal Center in the Chinese Academy of Sciences and housed at the Animal Science Center of Shanghai JiaoTong University, School of Medicine (SJTUSM). The animals were maintained under a 12 h light–dark cycle at 22°C. 60 rats were used to develop diabetes. The induction of diabetes was performed as described previously (Yang et al., 2016). In brief, 60 rats were fed with 60% high-fat diet (HFD) for 8 weeks. The rats were then fasted for 16 h, followed by multiple low-dose intraperitoneal injections of STZ (10 mg/kg body weight, dissolved in 0.1 mM citrate buffer) for 4 consecutive days. Rats were left to develop diabetes for 5 weeks. Random plasma glucose was measured, and a glucose level >300 mg/L was considered as diabetic. The remaining 30 rats were fed with a normal diet and were used as the normal control group (Norm). The characteristics of this diabetic model have been described in our previous work. In general, a combination of HFD feeding for 8 weeks and 4 consecutive days of low-dose STZ injections induced rats to develop type II diabetes with noticeable insulin

Journal of Cell Science (2020) 133, jcs235838. doi:10.1242/jcs.235838

resistance, persistent hyperglycemia, a moderate degree of insulinemia, as well as high serum cholesterol and triglyceride levels. The animal procedures were performed in accordance with the rules of the Animal Care Committee of SJTUSM, and all experimental protocols were approved by the SJTUSM Institutional Animal Care and Use Committee.

Wounding procedure

One day before wounding, each of 90 rats (30 healthy normal rats and 60 diabetic rats) were anesthetized with a single intraperitoneal injection of thiopental sodium (40 mg/kg body weight), the hairs on the back were shaved and thoroughly removed using Nair Hair remover lotion. On the day of wounding, the rats were anesthetized with thiopental sodium and a dose of tramadol. The animals were fixed on a hollow plank and the back was immersed in water at 80°C for 8 s to produce a 6×8 cm deep second-degree burn wound covering almost 20% total body surface area (TBSA). 8 ml saline was intraperitoneally injected for resuscitation immediately after injury. The diabetic rats were then randomly divided into two groups, the insulin group received 0.2 units insulin/2 ml saline through intrawound injection (DM+Ins) and the control group (DM) received 2 ml of saline injection every day. The healthy normal rats also received 2 ml saline every day after wounding until fully healed.

Measurement of wound closure: Rats were anesthetized with thiopental sodium at day 1, 4, 12, 16 and 20 after wounding. The wounds were photographed and drawn on transparent tracing paper. The wound sizes were analyzed using ImageJ software. The unhealed rate was calculated by comparing the unhealed wound area to the original wound area.

For the examination of IDE inhibition on diabetic wound healing: three healthy normal rats (Norm group) and six diabetic rats were allocated in this experiment. The diabetic rats were divided into two groups randomly (DM group and DM+IDE inhibitor group) after the preoperative preparation performed as described above. Each animal's back was punctured to produce six wounds of 1 cm diameter. IDE inhibitor 6bK (0.1 mg/ml dissolved in PBS) was used by intraperitoneal injection (80 mg/kg) for 3 consecutive days combined with 20 µl daily wound topical application until the wound healed. Wounds were photographed and drawn, as described above, on day 1, 4, 9 and 12 after wounding.

Histological observation

The wounds, including 5 mm adjacent normal skin, along with the subcutaneous fat tissue, were harvested at day 1, 4, 9 and 12 after wounding. The tissue was fixed in 4% paraformaldehyde and embedded in paraffin. Sections with ∼6–7 µm thickness were stained with Hematoxylin and Eosin (H&E) for histological and morphometric observation and evaluation. Masson Trichrome staining was used for collagen deposition evaluation.

Immunohistochemistry and immunofluorescence

The wounds were harvested and fixed as mentioned above, and sections were then deparaffinized, rehydrated and washed in distilled water. The sections were placed in ∼95–98°C antigen-retrieval citrate buffer (10 mM sodium citrate, pH 6) in a container for 10–15 min. Endogenous peroxidase activity was blocked by placing the sections in 3% hydrogen peroxide in methanol for 10 min. Non-specific staining was blocked with normal goat serum, and the sections were incubated with anti-rat IDE, CD66b and CD68 overnight at 4°C. After washing, HRP-labeled secondary antibody was applied for 1 h at room temperature, then samples were stained with diaminobenzidine, and counterstained with Hematoxylin.

TUNEL

TUNEL assays were performed as the instructions of Roche Applied Science. Dewaxed paraformaldehyde-fixed tissue sections were placed in a plastic jar containing 200 ml 0.1 M citrate buffer, pH 6.0. 750 W microwave irradiation was applied for 1 min. Samples were cooled rapidly by immediately adding 80 ml double distilled water. Slides were transferred to PBS, then immersed for 30 min in 0.1 M Tris-HCl, pH 7.5, containing 3% BSA and 20% normal bovine serum. Slides were rinsed twice with PBS. 50 µl of TUNEL reaction mixture was added to each section, then incubated for 60 mins at 37°C in a humidified atmosphere in the dark. Slides were rinsed three times in PBS for 5 min each, and then incubated with the neutrophil marker CD66b in a dark wet chamber overnight. Slides were then rinsed three times in PBS for 5 min each. The AlexaFluor 594-conjugated secondary antibody was added for 1 h, then slides were rinsed three times with PBS. Slides were mounted using Pro-Long anti-fade reagent with DAPI (Thermo Fisher) and then evaluated under a fluorescence microscope.

Immunofluorescence of isolated cells

Tissues were fixed in 4% paraformaldehyde at 4°C for 4 h followed by grade dehydration in 30, 20 and 10% sucrose for 30 min. The specimens were then embedded in OCT compound and stored at −80°C until use. The tissues were sectioned at 5 µm and placed on poly-L-lysine precoated slides. The slides were washed three times in PBS and then blocked in 5% BSA for 30 min at room temperature. Then, the primary antibodies (iNOS and CD68 for detection of M1 macrophages, CD68 and arginase 1 for detection of M2 macrophages, IR and IGFR combined with CD68 and CD66b for detection of IR and IGFR expression in neutrophils and macrophages) were incubated overnight at 4°C in a wet chamber. After washing with PBS three times, the samples were incubated with secondary antibodies conjugated with FITC or Rhodamine at room temperature for 1 h in a darkened wet chamber. Finally, the sections were washed with PBS three times and mounted with Pro-Long anti-fade reagent with DAPI. Tissues were observed under a fluorescence microscope (ZEISS) at a magnification of 40×.

Isolation of neutrophils and macrophages

Isolation of neutrophils and macrophages was performed as described previously (Swamydas et al., 2015). In brief, rats were injected intraperitoneally with 10 ml of 3% thioglycolate medium to induce sterile peritonitis. Peritoneal exudate cells were harvested by intraperitoneal injection of 10 ml of cold PBS or DMEM at 4 h and 3 days after thioglycolate injection for neutrophil and macrophage isolation, respectively. The isolation and purification of neutrophils and macrophages were then performed according to the following procedures. Neutrophils: the peritoneal exudate cells were centrifuged at 250 ***g*** for 10 min at 4°C and then resuspended in 10 ml of erythrocyte lysis buffer (6 mM NH_4Cl, 16.96 mM Tris, adjusted to pH to 7.2 with 1 M HCl) and incubated for 10 min at 37°C. Neutrophils were collected by centrifugation at 250 ***g*** for 10 min and resuspended in RPMI 1640 for further analysis. Macrophages: the harvested cells were cultured in the plates and left to adhere for 2 h. The non-adherent cells were washed with PBS three times and then cultured in DMEM with 10% FBS and PS for further analysis.

Neutrophil phagocytosis analysis

Neutrophils from the peritoneal cavity of both diabetic rats and normal rats were stimulated with FITC-labeled *E. coli* for 1 h. The culture medium was removed and washed. Cells were subjected to fluorescence microscope analysis. Neutrophil phagocytosis was observed when neutrophil uptake of FITC-labeled *E. coli* resulted in FITC-positive staining of the cell. Phagocytosis function index was calculated as the ratio of the number of neutrophils that had performed phagocytosis to the number of neutrophils that had not performed phagocytosis.

Phagocytosis-induced apoptotic neutrophil assays

Both normal and diabetic neutrophils were subjected to heat-killed *E. coli* stimulation. 18 h after stimulation, the cells were collected and lysed for apoptosis analysis. To assay the induction of macrophage polarization from M1 to M2 phenotype by apoptosed neutrophils, the neutrophils were collected from peritoneal cavities and cultured for 24 h. After confirming neutrophils were apoptosed, the apoptosed neutrophils were then collected and co-cultured with macrophages. Latex beads were used as a negative control for apoptosed neutrophils.

Wound cytokine array analysis

At 1, 4, 9 and 12 days after injury, the wound tissues were harvested and stored at −80°C. The tissue was homogenized by pulverization in liquid nitrogen and transferred to tissue lysis buffer with a protease inhibitor cocktail (Protease/Phosphatase Inhibitor Cocktail, Cell Signaling Technology,

catalog: 5872) followed by centrifugation at 13,400 ***g*** for 15 min. The supernatant was removed and used for cytokine array analysis on a sandwich ELISA rat cytokine array G2 preconfigured with 34 cytokines. The analysis was performed using the manufacturer's recommended protocol, and the signals of Cy3 were imaged using an Axon Gene Pix laser scanner (MDS analytical technologies, Sunnyvale, CA). Any ≥1.5-fold increase or ≤0.65-fold decrease in signal intensity groups was considered a measurable and significant difference in expression.

Western blotting

Tissues were homogenized by pulverization in liquid nitrogen and transferred to tissue lysis buffer with a Protease/Phosphatase Inhibitor Cocktail (Cell Signaling Technology, catalog: 5872), followed by centrifugation at 13,400 ***g*** for 15 min. The supernatants were removed and stored at −80°C. An equal amount of protein per lane (50 µg) was separated by 5–12% SDS–PAGE and transferred to a PVDF membrane. The membranes were blocked by 5% non-fat powdered milk in Tris-buffered saline with Tween-20 (TBST) and then incubated with anti-insulin, anti-IGF-1, anti-iNOS, anti-CD20, anti-IL-1β, anti-IR, anti-IGFR, anti-cleaved caspase-3 or anti-IL-10 primary antibodies in 5% non-fat milk in TBST overnight at 4°C. The membrane was then washed extensively with TBST and then incubated with the secondary antibody for 1 h at room temperature. Bands were visualized with enhanced chemiluminescence. Relative quantities of protein were determined using a densitometer and presented in comparison to β-actin expression.

Statistical analysis

Data analysis was performed using GraphPad Prism software (Graph Pad Software Inc.). *t*-tests were used to determine the significance of pairwise differences between means, unpaired *t*-tests were used for comparison between two groups and one-way ANOVA (Dunnett's post hoc test) were used to determine significance between means of several groups. Data were verified as satisfying the assumptions of ANOVA before performing the tests. $P<0.05$ was considered statistically significant, and $P<0.01$ was considered statistically highly significant. Data are shown as mean±s.d.

Competing interests

The authors declare no competing or financial interests.

Author contributions

Conceptualization: P.Y., X.Z., Y.L.; Methodology: X.W., D.W.; Software: M.Z., T.Y.; Formal analysis: Y.S.; Investigation: P.Y., X.W., D.W., D.L., M.G., Y.L.; Resources: T.Y.; Data curation: P.Y., Y.S., D.L.; Writing - original draft: P.Y.; Writing - review & editing: X.Z.; Visualization: M.Z.; Supervision: Y.L.; Project administration: X.Z., Y.L.; Funding acquisition: X.Z., Y.L.

Funding

This study is supported by the National Natural Science Foundation of China (81170761, 81270909, 81671914), Shanghai Hospital Development Center (SHDC12014117), Shanghai Municipal Key Clinical Specialty (shslczdzk02302), Shanghai Chinese and Western Medicine Clinical Cooperation Pilot Cultivation Project [ZY(2018-2020)-FWTX-1106], Ruijin Youth NSFC Cultivation Fund (2019QNPY01003) and Shanghai Jiao Tong University Medical Engineering Cross Research Funds (YG2019QNA35).

Supplementary information

Supplementary information available online at
https://jcs.biologists.org/lookup/doi/10.1242/jcs.235838.supplemental

References

Alba-Loureiro, T. C., Hirabara, S. M., Mendonca, J. R., Curi, R. and Pithon-Curi, T. C. (2006). Diabetes causes marked changes in function and metabolism of rat neutrophils. *J. Endocrinol.* **188**, 295-303. doi:10.1677/joe.1.06438

Allen, S. J., Crown, S. E. and Handel, T. M. (2007). Chemokine: receptor structure, interactions, and antagonism. *Annu Rev Immunol,* **25**, 787-820. doi:10.1146/annurev.immunol.24.021605.090529

American Diabetes, A. (2004). Diagnosis and classification of diabetes mellitus. *Diabetes Care* **27** Suppl. 1, S5-S10. doi:10.2337/diacare.27.2007.S5

Ariel, A. and Serhan, C. N. (2012). New lives given by cell death: macrophage differentiation following their encounter with apoptotic leukocytes during the resolution of inflammation. *Front Immunol* **3**, 4. doi:10.3389/fimmu.2012.00004

Baltzis, D., Eleftheriadou, I. and Veves, A. (2014). Pathogenesis and treatment of impaired wound healing in diabetes mellitus: new insights. *Adv. Ther.* **31**, 817-836. doi:10.1007/s12325-014-0140-x

Berbudi, A., Rahmadika, N., Tjahjadi, A. I. and Ruslami, R. (2020). Type 2 diabetes and its impact on the immune system. *Curr Diabetes Rev,* **16**, 442-449. doi:10.2174/1573399815666191024085838

Chen, X., Liu, Y. and Zhang, X. (2012). Topical insulin application improves healing by regulating the wound inflammatory response. *Wound Repair. Regen.* **20**, 425-434. doi:10.1111/j.1524-475X.2012.00792.x

Dovi, J. V., Szpaderska, A. M. and Dipietro, L. A. (2004). Neutrophil function in the healing wound: adding insult to injury? *Thromb. Haemost.* **92**, 275-280. doi:10.1160/TH03-11-0720

El Kebir, D. and Filep, J. G. (2010). Role of neutrophil apoptosis in the resolution of inflammation. *ScientificWorldJournal,* **10**, 1731-1748. doi:10.1100/tsw.2010.169

El Kebir, D. and Filep, J. G. (2013). Modulation of neutrophil apoptosis and the resolution of inflammation through β2 Integrins. *Front. Immunol.* **4**, 60. doi:10.3389/fimmu.2013.00060

Forbes, J. M. and Cooper, M. E. (2013). Mechanisms of diabetic complications. *Physiol. Rev.* **93**, 137-188. doi:10.1152/physrev.00045.2011

Fox, S., Leitch, A. E., Duffin, R., Haslett, C. and Rossi, A. G. (2010). Neutrophil apoptosis: relevance to the innate immune response and inflammatory disease. *J Innate Immun,* **2**, 216-227. doi:10.1159/000284367

Frydrych, L. M., Bian, G., O'lone, D. E., Ward, P. A. and Delano, M. J. (2018). Obesity and type 2 diabetes mellitus drive immune dysfunction, infection development, and sepsis mortality. *J Leukoc Biol,* **104**, 525-534. doi:10.1002/JLB.5VMR0118-021RR

Gurtner, G. C., Werner, S., Barrandon, Y. and Longaker, M. T. (2008). Wound repair and regeneration. *Nature* **453**, 314-321. doi:10.1038/nature07039

Headland, S. E. and Norling, L. V. (2015). The resolution of inflammation: principles and challenges. *Semin. Immunol.* **27**, 149-160. doi:10.1016/j.smim.2015.03.014

Kolaczkowska, E. and Kubes, P. (2013). Neutrophil recruitment and function in health and inflammation. *Nat. Rev. Immunol.* **13**, 159-175. doi:10.1038/nri3399

Lecube, A., Pachon, G., Petriz, J., Hernandez, C. and Simo, R. (2011). Phagocytic activity is impaired in type 2 diabetes mellitus and increases after metabolic improvement. *PLoS One* **6**, e23366. doi:10.1371/journal.pone.0023366

Leone, S., Pascale, R., Vitale, M. and Esposito, S. (2012). [Epidemiology of diabetic foot]. *Infez Med.* **20** Suppl. 1, 8-13.

Li, K. W., Turner, S. M., Emson, C. L., Hellerstein, M. K. and Dale, D. C. (2011). Deuterium and neutrophil kinetics. *Blood* **117**, 6052-6053. doi:10.1182/blood-2010-12-322271

Lima, M. H., Caricilli, A. M., De Abreu, L. L., Araujo, E. P., Pelegrinelli, F. F., Thirone, A. C., Tsukumo, D. M., Pessoa, A. F., Dos Santos, M. F., De Moraes, M. A. et al. (2012). Topical insulin accelerates wound healing in diabetes by enhancing the AKT and ERK pathways: a double-blind placebo-controlled clinical trial. *PLoS One* **7**, e36974. doi:10.1371/journal.pone.0036974

Liu, Y., Dhall, S., Castro, A., Chan, A., Alamat, R. and Martins-Green, M. (2018). Insulin regulates multiple signaling pathways leading to monocyte/macrophage chemotaxis into the wound tissue. *Biol Open* **7**, bio026187. doi:10.1242/bio.026187

Loffler, M. W., Schuster, H., Buhler, S. and Beckert, S. (2013). Wound fluid in diabetic foot ulceration: more than just an undefined soup? *Int. J. Low. Extrem. Wounds* **12**, 113-129. doi:10.1177/1534734613489989

Luo, H. R. and Loison, F. (2008). Constitutive neutrophil apoptosis: mechanisms and regulation. *Am. J. Hematol.* **83**, 288-295. doi:10.1002/ajh.21078

Mantovani, A., Biswas, S. K., Galdiero, M. R., Sica, A. and Locati, M. (2013). Macrophage plasticity and polarization in tissue repair and remodelling. *J. Pathol.* **229**, 176-185. doi:10.1002/path.4133

Martin, K. R., Ohayon, D. and Witko-Sarsat, V. (2015). Promoting apoptosis of neutrophils and phagocytosis by macrophages: novel strategies in the resolution of inflammation. *Swiss Med. Wkly.* **145**, w14056.

McCarty, S. M. and Percival, S. L. (2013). Proteases and delayed wound healing. *Adv Wound Care (New Rochelle)* **2**, 438-447. doi:10.1089/wound.2012.0370

McCracken, J. M. and Allen, L. A. (2014). Regulation of human neutrophil apoptosis and lifespan in health and disease. *J Cell Death* **7**, 15-23. doi:10.4137/JCD.S11038

Muller, M., Trocme, C., Lardy, B., Morel, F., Halimi, S. and Benhamou, P. Y. (2008). Matrix metalloproteinases and diabetic foot ulcers: the ratio of MMP-1 to TIMP-1 is a predictor of wound healing. *Diabet Med.* **25**, 419-426. doi:10.1111/j.1464-5491.2008.02414.x

Nunan, R., Harding, K. G. and Martin, P. (2014). Clinical challenges of chronic wounds: searching for an optimal animal model to recapitulate their complexity. *Dis Model Mech* **7**, 1205-1213. doi:10.1242/dmm.016782

Oldenborg, P. A. and Sehlin, J. (1998). Insulin-stimulated chemokinesis in normal human neutrophils is dependent on D-glucose concentration and sensitive to inhibitors of tyrosine kinase and phosphatidylinositol 3-kinase. *J. Leukoc. Biol.* **63**, 203-208. doi:10.1002/jlb.63.2.203

Ortega-Gómez, A., Perretti, M. and Soehnlein, O. (2013). Resolution of inflammation: an integrated view. *EMBO Mol Med* **5**, 661-674. doi:10.1002/emmm.201202382

Pierce, G. F. (2001). Inflammation in nonhealing diabetic wounds: the space-time continuum does matter. *Am. J. Pathol.* **159**, 399-403. doi:10.1016/S0002-9440(10)61709-9

Pillay, J., Den Braber, I., Vrisekoop, N., Kwast, L. M., De Boer, R. J., Borghans, J. A., Tesselaar, K. and Koenderman, L. (2010). In vivo labeling with 2H2O reveals a human neutrophil lifespan of 5.4 days. *Blood* **116**, 625-627. doi:10.1182/blood-2010-01-259028

Poon, I. K., Lucas, C. D., Rossi, A. G. and Ravichandran, K. S. (2014). Apoptotic cell clearance: basic biology and therapeutic potential. *Nat. Rev. Immunol.* **14**, 166-180. doi:10.1038/nri3607

Soehnlein, O. and Lindbom, L. (2010). Phagocyte partnership during the onset and resolution of inflammation. *Nat. Rev. Immunol.* **10**, 427-439. doi:10.1038/nri2779

Swamydas, M., Luo, Y., Dorf, M. E. and Lionakis, M. S. (2015). Isolation of mouse neutrophils. *Curr Protoc Immunol.* **110**, 3 20 1-3 20 15. doi:10.1002/0471142735.im0320s110

Tang, W. J. (2016). targeting insulin-degrading enzyme to treat type 2 diabetes mellitus. *Trends Endocrinol Metab,* **27**, 24-34. doi:10.1016/j.tem.2015.11.003

Tofts, P. S., Chevassut, T., Cutajar, M., Dowell, N. G. and Peters, A. M. (2011). Doubts concerning the recently reported human neutrophil lifespan of 5.4 days. *Blood* **117**, 6050-6052. doi:10.1182/blood-2010-10-310532

Walrand, S., Guillet, C., Boirie, Y. and Vasson, M.-P. (2004). In vivo evidences that insulin regulates human polymorphonuclear neutrophil functions. *J Leukoc Biol,* **76**, 1104-1110. doi:10.1189/jlb.0104050

Wilgus, T. A., Roy, S. and McDaniel, J. C. (2013). Neutrophils and wound repair: positive actions and negative reactions. *Adv. Wound Care* **2**, 379-388. doi:10.1089/wound.2012.0383

Wlaschek, M., Peus, D., Achterberg, V., Meyer-Ingold, W. and Scharffetter-Kochanek, K. (1997). Protease inhibitors protect growth factor activity in chronic wounds. *Br J Dermatol,* **137**, 646. doi:10.1111/j.1365-2133.1997.tb03804.x

Yang, P., Pei, Q., Yu, T., Chang, Q., Wang, D., Gao, M., Zhang, X. and Liu, Y. (2016). Compromised wound healing in ischemic type 2 diabetic rats. *PLoS One,* **11**, e0152068. doi:10.1371/journal.pone.0152068

Yano, H., Kinoshita, M., Fujino, K., Nakashima, M., Yamamoto, Y., Miyazaki, H., Hamada, K., Ono, S., Iwaya, K., Saitoh, D. et al. (2012). Insulin treatment directly restores neutrophil phagocytosis and bactericidal activity in diabetic mice and thereby improves surgical site Staphylococcus aureus infection. *Infect Immun,* **80**, 4409-4416. doi:10.1128/IAI.00787-12

Yu, T., Gao, M., Yang, P., Pei, Q., Liu, D., Wang, D., Zhang, X. and Liu, Y. (2017). Topical insulin accelerates cutaneous wound healing in insulin-resistant diabetic rats. *Am J Transl Res* **9**, 4682-4693.

Zhang, X.-J., Wu, X., Wolf, S. E., Hawkins, H. K., Chinkes, D. L. and Wolfe, R. R. (2007). Local insulin-zinc injection accelerates skin donor site wound healing. *J. Surg. Res.* **142**, 90-96. doi:10.1016/j.jss.2006.10.034